J. Hydrol. Hydromech., 71, 2023, 4, 464–474
https://doi.org/10.2478/johh-2023-0023
©2023 Saeid Okhravi et al., published by Sciendo. This work is licensed under the Creative Commons Attribution-NonCommercial-NoDerivatives 4.0 International Licence.

sciendo Journal of Hydrology and Hydromechanics Institute of Hydrology SAS

Flow resistance at lowland and mountainous rivers

Saeid Okhravi[1*], Mahdi Alemi[2], Hossein Afzalimehr[3], Radoslav Schügerl[1], Yvetta Velísková[1]

[1] Institute of Hydrology, Slovak Academy of Sciences, Dúbravská cesta 9, 84104, Bratislava, Slovak Republic.
[2] Departamento de Engenharia Civil, Faculdadede Engenharia, Universidade do Porto, Rua Dr. Roberto Frias, Porto 4200-465, Portugal.
[3] Department of Civil Engineering, Iran University of Science and Technology, Tehran 1311416846, Iran.
[*] Corresponding author. Tel.: +421-944624921. E-mail: saeid.okhravi@savba.sk

Abstract: This study initially examines the various sources of flow resistance in sand-bed (lowland) and gravel-bed (mountainous) rivers along with the limitations of traditional estimation methods. The nondimensional hydraulic geometry approach, relating dimensionless flow discharge (q^*) to the Darcy-Weisbach friction factor (f), has demonstrated good performance for both river types, covering shallow to moderately deep flows. However, accuracy in estimating f is affected by simplifications like assuming uniform and deep flow, neglecting bed load transport and vegetation effects, which require further evaluation. To address these issues, the proposed method is evaluated using data from four sand-bed rivers in Slovakia (with vegetation), and three gravel-bed rivers in Iran (dominated by cobbles and boulders). Bedforms prove to be significant resistance sources in all studied rivers. The approach yields separate predictors for each river type, showing a satisfactory agreement between observed and calculated values within a maximum deviation of ±20% error bands. These predictors are further validated using field data and established equations from rivers with similar physiographic characteristics. Results indicate the method performs well in predicting flow resistance in sand-bed rivers, slightly overestimating overall (+40%). It effectively captures riverbed features and vegetation influence under small-scale roughness conditions. However, the predictor's validity for gravel-bed rivers is somewhat limited due to high variability in water-surface profiles, making it challenging to accurately capture flow dynamics under large-scale roughness conditions. Addressing complex characteristics of gravel-bed riverbeds, including boulders and local energy extraction, is crucial for improving the estimation of water-surface profile variations and flow resistance using the hydraulic geometry approach.

Keywords: Flow resistance; Hydraulic geometry; Gravel-bed river; Sand-bed river; Field data; River engineering.

INTRODUCTION

Flow resistance in natural or engineered streams and/or rivers can arise from various features related to stream shape, topography, and bed texture (size distribution of sediment particles), which retard the flow, dissipate flow energy, and result in reduced flow velocity. The dissipation of flow energy occurs through two main processes in rivers. Firstly, energy loss occurs due to frictional forces induced by channel properties such as geometric shape, curvature, slope, and bottom morphology. This leads to a decrease in flow velocity as energy is consumed in generating downstream secondary flow, such as around bends or point bars. Secondly, the sediment transport process acts as an additional source of flow energy extraction (Dodangeh and Afzalimehr, 2022; Venditti, 2013). The loss of flow energy is accompanied by the generation of turbulence, where flow energy is converted into turbulent eddies. These eddies may grow initially but eventually dissipate into smaller vortices until the energy is dissipated through viscous forces as heat (Nezu and Nakagawa, 1993). Considering the dissipative nature of flow resistance, any element within a river that produces turbulence, including bed and bank roughness, bedforms, and vegetation, contributes to the overall flow resistance. It is important to note that the flow energy extracted by the channel's shape and scale is ultimately dissipated through turbulence, which transfers energy to friction within the bed and banks.

There are two primary sources of resistance to flow that are commonly recognized in natural rivers: skin friction f_S and form friction f_F. Skin friction arises from the frictional forces between individual grains on the bed and/or bank surfaces, while form friction is caused by river morphological features, specifically bedforms, which generate turbulence. The combined effect of these frictional forces determines the total flow resistance (f_T) (Dey, 2014; Vanoni and Brooks, 1957). Correspondingly, the total bed shear stress (τ_T) can be decomposed into skin shear stress (τ_S) and form shear stress (τ_F) (García, 2008).

The significance of each resistance type depends on the characteristics of the river, with f_S dominating in gravel-bed rivers and f_F prevailing in sand-bed rivers. Numerous studies have focused on quantifying bed shear stress induced by grain and form resistance separately (Afzalimehr et al., 2010; Einstein and Barbarossa, 1952; Garcia and Parker, 1993; Okhravi and Gohari, 2020; van Rijn, 1984; Wright and Parker, 2004; Yang et al., 2005). Venditti (2013) categorized methods for separating grain and form resistance into two general types. One method relies on empirical relations between grain-related shear stress and total shear stress (Afzalimehr et al., 2010; Einstein and Barbarossa, 1952; Wright and Parker, 2004). The other method utilizes bedform properties to determine the grain and form components of shear stress or related coefficients for calculating flow resistance (Garcia and Parker, 1993; van Rijn, 1984). The present study does not aim to provide an exhaustive explanation of the underlying approaches of these two methods but rather explores distinctive approaches that could be applied to calculate flow resistance in different river types, taking into account specific resistance sources in both lowland and highland (e.g., mountainous) rivers.

As briefly mentioned earlier, considerable attention has been devoted to understanding the primary sources of boundary resistance, including bedforms and grain sizes, in both lowland and mountainous rivers (Afzalimehr et al., 2010; Ferguson, 2007; Okhravi et al., 2022a; Powell, 2014; Yang et al., 2005). Rivers are typically classified based on their bed gradient and sediment size range. Gravel-bed rivers are predominantly found in mountainous regions with steep channels (gradient > 0.002 m/m) and are often characterized by a partial cover of coarse sediments, such as gravel, cobble, or boulder particles. On the other hand, sand-bed rivers or low-gradient rivers are characterized by a river bed dominated by sand-size particles (Schügerl et al., 2020; Sulaiman et al., 2017). However, in lowland areas, the presence of aquatic vegetation becomes a significant factor, particularly during the summer season, and must be considered as a resistance source (Cai et al., 2020; Champion and Tanner, 2000; Mewis, 2021; Okhravi et al., 2022a; Song et al., 2014, 2017). Among the physical and environmental factors influencing vegetation accumulation in lowland rivers (e.g., river management practices, bed texture, nutrient and light availability, and flow conditions), Franklin et al. (2008) emphasized that flow velocity has the most significant impact. In other words, flow velocity directly influences flow resistance, making water depth (h), hydraulic radius (R), flow velocity (u), cross-sectional area of flow (A), and shear stress (τ) essential parameters for geomorphological assessments and modeling. Several well-established flow resistance equations, such as the Chezy and Darcy-Weisbach expressions, as well as the Manning formula, are widely used and do not require calibration for uniform flow conditions within a river reach (Amiri et al., 2016; Okhravi, 2022).

$$u = \frac{1}{n} R^{2/3} S^{1/2} = C\sqrt{RS} = \sqrt{\frac{8gRS}{f}} = u_* \sqrt{\frac{8}{f}} \tag{1}$$

where u is the mean flow velocity (LT^{-1}), C is the Chezy coefficient ($L^{1/2}T^{-1}$), n is the Manning coefficient ($L^{-1/3}T$), f (dimensionless) is the Darcy-Weisbach friction factor, S is the energy slope, R is the hydraulic radius (L) and g is the acceleration due to gravity (LT^{-2}). It is worth noting that the term $\sqrt{gRS}$ in Eq. (1) has the dimension LT^{-1}, which corresponds to a velocity term commonly known as the shear velocity and denoted as u_*.

All forms of Eq. (1) use a resistance coefficient, and the primary challenge with using these equation forms is their dependence on scale (Namaee et al., 2017; Venditti, 2013). This implies that resistance coefficients calculated for small to medium-sized channels or streams may not be suitable for large rivers, even if they belong to the same morphological catchment. Additionally, within a specific river, flow resistance varies significantly across different reaches at a given discharge (Ferguson et al., 2017). This poses a significant barrier when modeling river systems using a constant resistance coefficient, even with calibration, and it has adverse implications for numerous hydrological and hydro-morphological applications (Okhravi, 2022; Thomas et al., 2023). Moreover, flow resistance changes with variations in flow discharge; as flow discharge and depth increase, both the Manning coefficient and the Darcy-Weisbach friction factor decrease (Ferguson et al., 2017). Furthermore, the development of n and f based on the assumption of uniform flow limits the applicability of these equations since non-uniform flow conditions prevail in most rivers. These are the general limitations that pertain to Eq. (1), while there are also specific limitations that are relevant to lowland and mountainous rivers.

In addition to the general limitations associated with using Eq. (1), Ferguson (2010) conducted a series of analyses using extensive field data sets. The results provided evidence of the Manning equation's inaccurate predictions of flow resistance in certain conditions, such as steep and small rivers, shallow flows, and the presence of vegetation and bedforms, despite its widespread popularity. For instance, Okhravi et al. (2022a) highlighted that the fixed values of n and f are not suitable for mobile river beds (e.g., sand-bed rivers) or lowland rivers that undergo time-dependent changes in vegetation patches along the banks and bed. Previous studies revealed flaws in the Manning and Darcy-Weisbach equations when predicting flow resistance for relative submergence $R/d_{84} < 10$ (d_{84} represents the 84% finer grain size) in both types of rivers (Ferguson, 2010; Namaee et al., 2017), particularly in gravel-bed rivers (Ferguson et al., 2017). In high-gradient gravel-bed rivers, the relative submergence typically remains significantly below 10 and sometimes approaches values close to 1. In such cases, the differentiation between grain and form resistance becomes less distinct, as individual grains contribute to substantial form drag, and a significant amount of momentum is dissipated through the formation of wakes (D'Agostino and Michelini, 2015; Nicosia et al., 2023). Ferguson (2007) established a relationship between flow resistance (expressed as $(8/f)^{0.5}$) and relative submergence (R/d_{84}) in coarse-bed rivers through a proposed variable-power equation (VPE), as follows:

$$\frac{u}{u_*} = \sqrt{\frac{8}{f}} = \frac{a_1 a_2 (R/d_{84})}{\sqrt{a_1{}^2 + a_2{}^2 (R/d_{84})^{1.67}}} \tag{2}$$

in which $a_1 = 6.5$ and $a_2 = 2.5$ (Ferguson, 2007), are suitable for a wide range of submergence conditions in natural rivers. Ferguson (2007), Rickenmann and Recking (2011), and Ferguson et al. (2017) have mathematically demonstrated that a nondimensional hydraulic geometry equation, represented by $u^{**} \propto q^{*}$ is a form of VPE, where $q^{*} = q/\sqrt{g d_{84}{}^3 S}$ and $u^{**} = u/\sqrt{g d_{84} S}$, and q represents the discharge per unit channel width. Ferguson (2007) demonstrated that the power function provides a better fit between u^{**} and q^{*} compared to other functions and equations. The analyses conducted by Rickenmann and Recking (2011), Namaee et al. (2017), and Mendicino and Colosimo (2019) have shown that the flow discharge-based version of the VPE provides an accurate fit for the compiled data.

The nondimensional hydraulic geometry approach has proven effective in predicting flow resistance by connecting the Darcy-Weisbach friction factor (f) with velocity distribution, based on the universal velocity distribution law (Afzalimehr et al., 2011; Naderi et al., 2022; Yen, 2002). Okhravi et al. (2022a) successfully applied this approach, using flow discharge as an input, to sand-bed rivers with aquatic vegetation. In this study, we aim to evaluate the applicability of the nondimensional hydraulic geometry approach to gravel-bed rivers characterized by large particles and macrotopographic bedforms, where sediment transport is negligible. To support our main argument, we analyze the variations of flow resistance with flow discharge in different short reaches of the studied rivers. We validate the accuracy of the results obtained by separate predictors for both river types in lowland (sand-bed rivers) and mountainous (gravel-bed rivers) areas using field data and established formulas. We also propose modifications to the predictors as necessary. The findings of this study facilitate a more streamlined calibration process for hydrodynamic and

morphodynamic models, enhancing the performance of hydraulic models by accurately predicting hydraulic characteristics and shear stress for sediment transport modeling. These predictions are based on the distinct hydraulic and sediment characteristics that govern each river type.

METHODOLOGY FRAMEWORK

As mentioned earlier, the assumption of uniform flow cannot be applied to rivers, particularly in mountainous regions, due to bed irregularities and significant variations in flow depth. To account for flow non-uniformity when predicting flow resistance, it is recommended to estimate the shear velocity using the log law, particularly for small-scale roughness ($h/d_{84} > 4$) (Afzalimehr and Rennie, 2009; Powell, 2014). Furthermore, Afzalimehr (2010) found a strong correlation between shear velocity values estimated by the log law and Reynolds shear stresses in gravel-bed rivers. Hence, the shear velocity can be determined using the two-point velocity method proposed by Julien (1995) in Eq. (3), while the total friction factor is determined by the relationship $f = 8(u_*/u)^2$.

$$\frac{u_{f2}-u_{f1}}{u_*} = \frac{1}{\kappa}(\ln y_2 - \ln y_1) \;\Rightarrow\; u_* = \frac{\kappa\,(u_{f2}-u_{f1})}{\ln(\frac{y_2}{y_1})} \tag{3}$$

where κ is the von Kármán coefficient which remains constant ($\kappa \approx 0.4$) over semi-rigid boundary e.g., an armored river bed in a gravel bed river, and u_{f1} and u_{f2} are local flow velocity values at 20% and 80% of the flow depth from the water surface in a velocity profile, respectively, along with vertical distances y_1 and y_2 of these points from the water surface. However, it is important to note that this method is not recommended for sand-bed rivers when sediment entrainment occurs, as the log law exhibits a decrease in the von Kármán constant (Dey, 2014; Malakar and Das, 2021). Numerous studies have demonstrated that flow resistance is enhanced by sediment-laden flow, resulting in reduced flow velocity and an increase in the ratio of bed-roughness scale to the moving sediment layer (Ferro, 2018b; Mendicino and Colosimo, 2019). In the case of the selected sand-bed streams in this study, the variations in flow depth are not significant due to the very low bed slope, fewer cross-section irregularities, and a homogeneous layer of fine, uniform sediment. As a result, shear velocity was computed using the cross-sectionally averaged flow depth and the reach-scaled averaged slope of the bed.

As previously mentioned, Okhravi et al. (2022a) employed a nondimensional hydraulic geometry approach (Eq. (4)) specifically for sand-bed rivers. In this approach, the dimensionless mean flow velocity (u^{**}) is correlated with the dimensionless unit discharge (q^*), with a modification compared to Ferguson's (2007) approach for gravel-bed rivers. Instead of using the d_{84} parameter, Okhravi et al. (2022a) substituted it with the hydraulic radius (R) and obtained promising results. Sand-bed rivers are characterized by high relative submergence and very small-scale roughness (Franklin et al., 2008; Sulaiman et al., 2017), where the primary sources of flow resistance are bedforms and vegetation, rendering grain size irrelevant in this context (Okhravi et al., 2022a).

$$u^{**} = bq^{*m},\; u^{**} = u/\sqrt{gRS} \text{ and } q^* = q/\sqrt{gR^3S} \tag{4}$$

In Eq. (4), the coefficients b and m are determined empirically. The dimensionless discharge (q) represents the ratio of flow discharge (Q) to channel width (B). Eq. (4) can be used to calculate the friction factor (f) when considering the hydraulic characteristics of the flow, such as velocity (u), hydraulic radius (R), discharge (Q), and the channel slope (S). The inclusion of the channel slope accounts for variations in the water surface. The goal of this study was to apply the nondimensional hydraulic geometry approach based on Eq. (4) to gravel-bed rivers and compare the results with the original approach proposed by Ferguson (2007) as well as other relevant field data sets and developed formulas.

Statistical analysis was conducted to assess the agreement between the calculated and observed values of the dimensionless mean flow velocity (u^{**}). Measures such as the determination coefficient (r^2 or r-squared, Eq. (5)), root mean square error (RMSE, Eq. (6)), scatter index (SI), and index of agreement (I_a) were used for this purpose. It is worth noting that I_a proved to be a valuable metric for evaluating the similarity between observed and computed data by appropriately considering errors and differences (Eslamian et al., 2019; Okhravi et al., 2022b). Optimal agreement is indicated by a value of unity for I_a, while a close-to-zero RMSE signifies the best fit between observed and computed values (Willmott et al., 2012). Additional evaluation measures employed were percent bias (PBIAS) and the Nash-Sutcliffe model efficiency coefficient (NSE). PBIAS indicates the average tendency of computed values relative to observed values, with zero being the optimum value. Positive PBIAS indicates overestimation, while negative PBIAS indicates underestimation (Alemi and Maia, 2022). NSE is a favored statistic for assessing the predictive performance of hydrological models, with higher values indicating greater predictive accuracy. A perfect fit corresponds to an NSE value of unity (NSE = 1). The formulas for these evaluation parameters are as follows:

$$r^2 = \left(\frac{\sum_{i=1}^{N}(x_{o,i}-\bar{x}_{o,i})(x_{c,i}-\bar{x}_{c,i})}{\sqrt{\sum_{i=1}^{N}(x_{o,i}-\bar{x}_{o,i})^2}\cdot\sqrt{\sum_{i=1}^{N}(x_{c,i}-\bar{x}_{c,i})^2}} \right)^2 \tag{5}$$

$$\mathrm{RMSE} = \sqrt{\frac{\sum_{i=1}^{N}(x_{o,i}-x_{c,i})^2}{N}} \tag{6}$$

$$\mathrm{SI} = 100\,\frac{\sqrt{(1/N)\sum_{i=1}^{N}(x_{o,i}-x_{c,i})^2}}{\bar{x}_{o,i}} \tag{7}$$

$$I_a = 1 - \frac{\sum_{i=1}^{N}(x_{o,i}-x_{c,i})^2}{\sum_{i=1}^{N}\left(|x_{o,i}-\bar{x}_{o,i}|+|x_{c,i}-\bar{x}_{o,i}|\right)^2} \tag{8}$$

$$\mathrm{PBIAS} = 100\,\frac{\sum_{i=1}^{N}(x_{o,i}-x_{c,i})}{\sum_{i=1}^{N}x_{o,i}} \tag{9}$$

$$\mathrm{NSE} = 1 - \frac{\sum_{i=1}^{N}(x_{o,i}-x_{c,i})^2}{\sum_{i=1}^{N}(x_{o,i}-\bar{x}_{o,i})^2} \tag{10}$$

In the aforementioned equations, the variables x_o and x_c represent the observed and computed values, respectively. The variables $\bar{x}_o$ and $\bar{x}_c$ denote the average values of the observed and calculated data, respectively. N represents the number of samples.

Hydraulic assumptions about flow resistance in both river types

Following the description of the analytical methodology and preceding the discussion of field investigations, this study outlines the fundamental assumptions that underlie the hydraulic geometry approach used for predicting flow resistance.

The nondimensional hydraulic geometry approach has demonstrated its effectiveness in predicting flow resistance for rivers with varying characteristics. It has been particularly successful in lowland rivers that feature low-gradient sand-sized channels, high relative submergence (with $R/d_{84} > 10$ or even >100), relatively uniform and quasi-steady flow, low sediment transport, and seasonal changes in vegetation. Several studies, such as Song et al. (2017), Cai et al. (2020), and Okhravi et al. (2022a) have validated the performance of the hydraulic geometry approach in these river types.

For sand-bed rivers, the flow resistance equations developed based on the hydraulic geometry approach are particularly recommended. These equations account for the presence of lower regime flow bedforms, such as dunes and ripples, as well as aquatic vegetation (Okhravi et al., 2022a). In gravel-bed rivers, where flow discharge plays a crucial role in channel formation and is responsible for bed topography irregularities and water level fluctuations, hydraulic geometry equations provide a good representation of flow resistance across a range of flow depths, from shallow to moderately deep flows. This is observed despite the presence of the Manning's equation and logarithmic resistance relation. Previous studies conducted by Ferguson (2007), Ferguson et al. (2017), and Rickenmann and Recking (2011) have supported the application of hydraulic geometry equations in gravel-bed rivers.

Gravel-bed rivers are known for their typically high velocities and significant sediment transport, especially under upper regime flow conditions. However, in our study, we deliberately selected downstream armored reaches of gravel-bed rivers that exhibit low sediment transport and negligible bed load transport. This deliberate selection enables us to confidently apply the hydraulic geometry approach in analyzing flow resistance within these specific reaches. By focusing on these reaches with reduced sediment transport, we can effectively utilize the hydraulic geometry approach to study flow resistance in a more controlled and representative manner.

FIELD INVESTIGATIONS

The data for this study was extracted from the research conducted by Okhravi and Gohari (2020), focusing on three gravel-bed rivers in central Iran: the Kaj, the Zayandehrood, and the Marbar River. The selected reaches within each river were chosen to represent a sequence of pool and riffle formations, as well as microtopographic clusters, which are common bedforms in gravel-bed rivers. To collect velocity data, vertical velocity profiles were measured at the center of the river and near the banks using a propeller current meter with an accuracy of 2.5%.

The mean local flow velocity (u_f) was then determined by averaging the measured velocities at $0.2h$ and $0.8h$ from the water surface using the formula $u_f = (u_{f\,0.2} + u_{f\,0.8})/2$. Table 1 provides information on the 24 sections selected in the three gravel-bed rivers for this study, denoted as A, B, and C. The table includes details about the substrate materials forming the riverbed as well as the hydraulic flow conditions at each section.

The characteristics of riverbeds in gravel-bed rivers are more complex compared to sand-bed rivers found in lowland catchments. Sand-bed rivers typically consist of a narrow range of particle sizes, resulting in uniform sediment where the d_{50} (median grain size) is predominantly transported as suspended load. In contrast, gravel-bed rivers contain a wide range of particle sizes, ranging from fine sediment to cobbles and boulders, creating non-uniform sediment conditions. Due to

Table 1. Hydraulic and sediment parameters: measurements and calculations in three gravel-bed rivers.

Reach Name	Sections	S (–)	h (m)	u (m/s)	u_* (m/s)	d_{50} (mm)	d_{84} (mm)	Q (m^3/s)	τ [a] (pa)	Fr [b] (–)	f (–)	h/d_{84} (–)
	A1	0.0015	0.33	0.81	0.072	29.3	45.6	3.02	5.17	0.45	0.063	7.23
Zayandehrood	A2	0.0011	0.42	0.67	0.067	54.66	121.3	2.56	4.53	0.33	0.081	3.47
	A3	0.0011	0.34	0.706	0.062	39	96.25	2.71	3.83	0.38	0.061	3.53
	B1	0.003	0.43	0.545	0.0484	23	41.54	5.45	2.34	0.27	0.063	10.35
	B2	0.0025	0.42	0.867	0.097	50	71.3	6.04	9.36	0.43	0.1	5.89
	B3	0.0041	0.43	1.204	0.1137	17.5	21.7	7.13	12.93	0.59	0.071	19.82
Kaj	B4	0.0028	0.33	1.23	0.1457	42.5	51	5	21.23	0.69	0.112	6.47
	B5	0.006	0.36	1.05	0.1027	42.5	54	8.5	10.55	0.56	0.077	6.66
	B6	0.002	0.55	1.06	0.097	35	56.87	7.28	9.41	0.45	0.067	9.67
	B7	0.0081	0.54	0.581	0.066	25	43.3	4.66	4.38	0.25	0.104	12.47
	B8	0.0026	0.3	0.761	0.1075	23	38.75	5.42	11.55	0.44	0.16	7.75
	B9	0.0026	0.33	0.932	0.093	50	69	9.16	8.65	0.52	0.08	4.78
	C1	0.0064	0.26	1.206	0.1285	40	55	9.64	16.52	0.75	0.091	4.72
	C2	0.0086	0.16	1.01	0.1175	35	55	7.48	13.81	0.8	0.11	2.91
	C3	0.0051	0.19	0.928	0.0962	35	55	6.14	9.253	0.69	0.086	3.45
	C4	0.0016	0.68	1.203	0.1033	35	75	6.42	10.66	0.47	0.059	9.1
	C5	0.0094	0.36	1.334	0.1825	18	35	8.77	33.31	0.71	0.15	10.28
Marbar	C6	0.0038	0.29	0.658	0.1041	35	55	5.39	10.84	0.39	0.2	5.27
	C7	0.0055	0.36	0.85	0.139	65	105	8.89	19.3	0.45	0.214	3.43
	C8	0.0043	0.32	1.012	0.1163	21	40	7.74	13.53	0.57	0.106	8
	C9	0.0021	0.52	0.702	0.1032	55	75	5.72	10.66	0.31	0.173	6.93
	C10	0.0022	0.48	0.64	0.1034	50	65	5.48	10.71	0.3	0.209	7.38
	C11	0.0012	0.32	0.735	0.0627	16	30	3.67	3.93	0.41	0.058	10.67
	C12	0.0002	0.9	0.542	0.0477	55	75	2.88	2.27	0.18	0.062	12

[a] τ is the shear stress at the bed.
[b] Fr is the Froude number.

the lower relative submergence in gravel-bed rivers, the d_{50} is transported mostly as bed load (Sulaiman et al., 2017). As a consequence of the sediment non-uniformity, different particle size fractions in a gravel-bed river are transported at varying rates. Finer particles are transported more rapidly, leading to the coarsening of the riverbed surface. This gradual process results in the development of a larger and more stable surface texture, commonly known as an armor layer. However, if a higher velocity flow occurs, it can disrupt the armor layer. Therefore, the selective transport of different particle size fractions contributes to the complexity of gravel-bed river features (Okhravi and Eslamian, 2022). Diplas et al. (2016) observed that the ratio of $d_{max}/d_{50} > 7.5$, where d_{max} represents the coarsest particle size, and indicates the most significant coarsening state of the bed-armoring.

This study also incorporates data from four lowland streams, primarily composed of sand-bed channels, situated in the western part of Slovakia near the city of Bratislava (Table 2). Detailed information regarding the geomorphology, sediment characteristics, and flow conditions of these four streams has been previously discussed in Okhravi et al. (2022a). These streams predominantly consist of sand-sized particles and exhibit low slopes, resulting in lower-regime flows characterized by relatively low velocities and sediment transport. The prevalent bedforms in these streams are typically dunes or ripples, which contribute significantly to form resistance (Okhravi et al., 2022a; Zomer et al., 2023). Furthermore, the presence of vegetation can introduce additional resistance, emphasizing the importance of incorporating vegetation in predictive flow resistance methods (Box et al., 2021; Willemsen et al., 2022). The coverage of vegetation in the surrounding area varies over time, with higher abundance during low summer flows directly increasing flow resistance. The variations in flow discharge can also influence the temporal dynamics of vegetation patches and bedforms (Okhravi et al., 2022a; Song et al., 2017). Table 2 provides the field data and measured values of hydraulic characteristics for 45 cross-sections obtained during a period of moderate water level (June). Fig. 1 showcases different views of gravel-bed and sand-bed rivers investigated in this study, representing both mountain and lowland catchments in Iran and Slovakia, respectively.

Table 2. Hydraulic and sediment parameters: measurements and calculations in four sand-bed rivers.

Reach Name	Sections	S (–)	h (m)	u (m/s)	u_* (m/s)	Q (m^3/s)	τ (Pa)	Fr (–)	f (–)
	D1	0.0002	0.56	0.13	0.033	0.39	1.1	0.06	0.50
Malina	D2	0.0002	0.52	0.14	0.034	0.37	1.19	0.06	0.461
	D3	0.0003	0.6	0.14	0.038	0.51	1.43	0.06	0.557
	D4	0.0003	0.75	0.086	0.042	0.48	1.8	0.03	1.937
	E1	0.0004	0.1	0.2	0.02	0.085	0.39	0.2	0.08
Šúrsky	E2	0.0004	0.42	0.05	0.037	0.097	1.43	0.025	4.591
	E3	0.0003	0.47	0.037	0.037	0.1	1.4	0.02	8.216
	E4	0.0003	0.35	0.03	0.032	0.11	1.02	0.02	9.716
	F1	0.00003	1.21	0.084	0.021	2.05	0.46	0.024	0.524
	F2	0.00004	1.09	0.097	0.02	1.93	0.42	0.03	0.354
	F3	0.00001	1.04	0.118	0.012	2.02	0.14	0.037	0.081
	F4	0.00004	1.05	0.1	0.006	1.92	0.04	0.031	0.032
	F5	0.00004	0.99	0.112	0.02	1.74	0.42	0.036	0.266
	F6	0.00004	0.6	0.17	0.017	1.82	0.26	0.07	0.071
	F7	0.00003	0.83	0.118	0.016	1.76	0.26	0.041	0.149
	F8	0.00009	0.63	0.165	0.025	1.9	0.60	0.066	0.177
	F9	0.00003	0.7	0.128	0.014	1.3	0.21	0.049	0.101
Gabčíkovo	F10	0.00013	0.74	0.155	0.03	1.82	0.91	0.058	0.301
Topoľníky	F11	0.00019	0.68	0.137	0.027	1.67	0.73	0.052	0.309
	F12	0.00004	0.67	0.126	0.017	1.45	0.3	0.049	0.152
	F13	0.00009	0.72	0.132	0.025	1.57	0.64	0.05	0.295
	F14	0.00008	1.07	0.139	0.029	1.33	0.83	0.043	0.344
	F15	0.00015	0.53	0.128	0.028	0.89	0.78	0.056	0.378
	F16	0.00006	1.14	0.08	0.008	1.57	0.06	0.024	0.081
	F17	0.00002	0.89	0.093	0.014	1.58	0.21	0.031	0.193
	F18	0.00004	1.06	0.076	0.006	1.15	0.04	0.024	0.057
	F19	0.00037	0.74	0.118	0.016	1.45	0.27	0.044	0.153
	F20	0.00003	0.53	0.138	0.011	1.46	0.13	0.061	0.054
	F21	0.00003	0.51	0.158	0.011	1.35	0.12	0.071	0.036
	F22	0.00014	0.76	0.288	0.032	2.62	1.04	0.105	0.101
	F23	0.00014	1.08	0.148	0.038	2.38	1.47	0.046	0.536
	G1	0.00002	1.3	0.139	0.014	3.06	0.19	0.039	0.079
	G2	0.00002	1.35	0.14	0.014	2.8	0.2	0.038	0.082
	G3	0.00003	1.01	0.133	0.017	2.69	0.29	0.042	0.131
	G4	0.00008	0.99	0.174	0.028	2.89	0.79	0.056	0.208
	G5	0.00008	1.02	0.172	0.028	2.81	0.81	0.054	0.218
	G6	0.00001	0.87	0.222	0.01	3.03	0.11	0.076	0.018
Chotárny	G7	0.00001	0.81	0.201	0.01	2.81	0.1	0.071	0.021
	G8	0.00012	0.95	0.206	0.033	3.09	1.08	0.066	0.205
	G9	0.00007	1.01	0.183	0.027	2.89	0.7	0.058	0.167
	G10	0.00005	0.95	0.203	0.007	3.36	0.05	0.066	0.009
	G11	0.00005	0.95	0.198	0.007	3.12	0.05	0.065	0.009
	G12	0.00003	0.9	0.167	0.017	2.66	0.3	0.056	0.086
	G13	0.00003	0.71	0.195	0.015	2.49	0.24	0.074	0.049
	G14	0.00004	0.66	0.209	0.016	2.38	0.27	0.082	0.05



Fig. 1. Typical views of gravel-bed and sand-bed rivers. Selected photos from top-left to bottom-left showcase gravel-bed rivers in central Iran ([a] Kaj [32.1116 °N and 50.5045 °E] and [b] Zayandehrood [32.3742 °N and 51.2135 °E] Rivers), while photos from top-right to bottom-right depict sand-bed rivers in western Slovakia ([c] Gabčíkovo-Topoľníky [47.8937 °N and 17.5509 °E] and [d] Chotárny [47.8396 °N and 17.6125 °E] engineered rivers).

RESULTS

The objective of the current study was to develop flow resistance predictors that encompass the primary factors influencing boundary resistance in both river types, including bed grains, bedforms, and vegetation. The investigations demonstrated the efficacy of the proposed framework in predicting flow resistance for sand-bed rivers in lowland areas, as evidenced by the connections established between flow characteristics and the dimensionless mean flow velocity (u^{**}) with flow resistance factor f via Eq. (4) (Okhravi et al., 2022a). Consequently, it is natural to inquire about the applicability of this approach to gravel-bed rivers.

To develop a flow resistance predictor based on the framework of Eq. (4), field data from gravel-bed rivers were utilized. This data, as presented in Table 1, follows a similar structure to the data already employed for sand-bed rivers in Table 2. The nondimensional hydraulic geometry approach utilizes flow discharge as an input parameter, establishing its connection with velocity distribution and, consequently, with flow resistance f. Eq. (4) was independently applied to the field data for both gravel-bed and sand-bed rivers, yielding the following power-form equations (Eqs. (11) and (12)) for each river type. It is important to note that these equations explicitly account for flow non-uniformity by incorporating the slope of energy grade lines (friction slope) and indirectly incorporating flow discharge and velocity profiles.

$$\text{For gravel-bed rivers,} \quad u^{**} = 2.05 q^{*0.668} \tag{11}$$

$$\text{For sand-bed rivers,} \quad u^{**} = 0.978 q^{*0.953} \tag{12}$$

The scatter plot of u^{**} and q^{*} is depicted in Fig. 2. It is important to note that seven outliers from the gravel-bed rivers in the Kaj River (Table 1) were excluded from the regression analysis (Fig. 2a). The coefficient of determination indicates the correlations between u^{**} and q^{*}, revealing a better fit for sand-bed rivers using Eq. (12) (r^2 = 0.97) compared to gravel-bed

rivers using Eq. (11) ($r^2 = 0.74$). The statistical analysis involved comparing the calculated values of u^{**} using Eqs. (11) and (12) with the corresponding observed values in the field, as illustrated in Fig. 3. The figure demonstrates the strong performance of the predictors, indicated by high values of the index of agreement (I_a) and Nash-Sutcliffe efficiency coefficient (NSE), as well as low values RMSE, SI, and PBIAS. The low values of PBIAS, approaching zero, indicate that the model results align closely with the observed values, irrespective of overestimation for gravel-bed rivers' data (Fig. 3a) and underestimation for sand-bed rivers' data (Fig. 3b). Consistent with the explanations regarding PBIAS, the low values of normalized RMSE (NRMSE = RMSE/$\bar{x}_o$ = 0.11 for gravel-bed rivers and 0.13 for sand-bed rivers) for the observed data confirm the minimal errors of the flow resistance predictors (with an optimal NRMSE value of zero). The value of NSE reflects the excellent performance of Eq. (12) for sand-bed rivers, while the predictor for gravel-bed rivers demonstrates a lower NSE of 0.74, which is still considered good based on criteria established by Allen et al. (2007), Moriasi et al. (2015), and Alemi and Maia (2022) for various ecosystems and hydrologic conditions. Overall, the proposed method exhibits relatively lower performance for gravel-bed rivers due to the high variability of energy slope (S) in each section. The variability in S is characteristic of mountainous rivers (Zwolenik and Michalec, 2023) with high flow velocity and significant irregularities in cross-sections, including the sudden presence of large cobbles or boulders on the river bed.

To evaluate the accuracy of the predicted u^{**} values, error bands were plotted in Fig. 3 relative to the perfect agreement line. The results indicate that over 80% of the calculated u^{**} values fall within the ±20% and ±10% error bands for sand-bed rivers and gravel-bed rivers, respectively. This trend demonstrates that when river features and catchment characteristics are more similar, there is less scatter around the ideal line, resulting in higher predictor performance. The satisfactory agreement observed between the predicted u^{**} values using Eq. (11) and the observed values in gravel-bed rivers is particularly encouraging. This agreement is significant because the shear velocity was calculated using Eq. (3), which applies the log law and takes into consideration velocity profiles and boundary-layer characteristics. Consequently, Eq. (11) effectively addresses non-uniform flow conditions in gravel-bed rivers and accurately determines the flow resistance coefficient f.

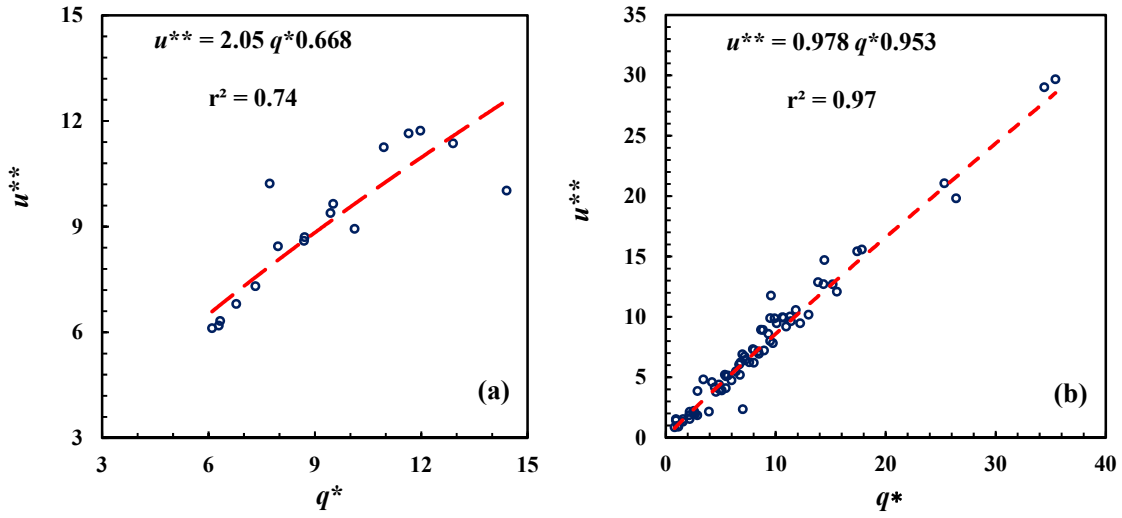


Fig. 2. The correlation between u^{**} and q^{*} in (a) gravel-bed rivers and (b) sand-bed rivers.

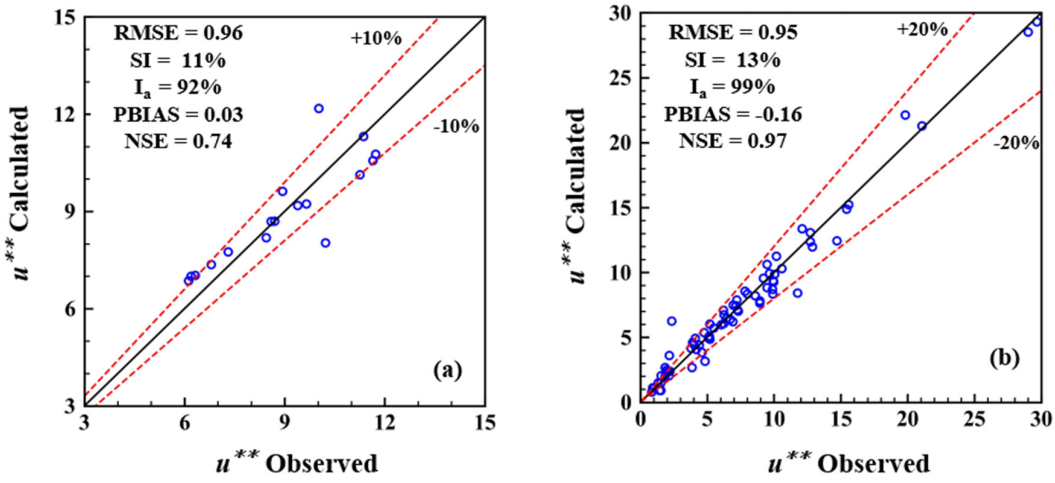


Fig. 3. The statistical evaluation of u^{**} using Eqs. (11) and (12), compared to field measurements in (a) gravel-bed rivers and (b) sand-bed rivers.

As mentioned earlier, the original formulation of Eq. (4) proposed by Ferguson (2007) used d_{84} instead of R ($q^* = q/\sqrt{g{d_{84}}^3 S}$ and $u^{**} = u/\sqrt{gd_{84}S}$,). In an attempt to explore alternative equations, the available datasets were used to derive an equation based on the original formulation and compare it with the outcomes obtained using Eq. (11). However, it was observed that the correlation between u^{**} and q^* using d_{84} in the selected reaches was found to be quite weak. This was mainly due to significant variations in the grain size distribution of the bed, with d_{84} ranging from 20 to 125 mm, while the ratio of h/d_{84} varied between 2 and 20. Furthermore, the selected reaches were characterized by armoring and the presence of particle clusters, leading to substantial variability in material distribution across the surface and subsurface of the river bed. Therefore, it is recommended to utilize a flow depth-based version of the VPE that captures the variations in velocity with depth and accurately represents the flow resistance behavior along the bed section.

DISCUSSION

Previous literature on widely-used equations for predicting flow resistance, such as the one presented in Eq. (1), has demonstrated several limitations and disadvantages. For instance, these equations are not suitable for non-uniform flow and cannot account for variations in vegetation coverage and bed load transport in lowland rivers (Dingman, 2009; Ferguson, 2010; Ferguson et al., 2022; Mendicino and Colosimo, 2019). Consequently, it is evident that these equations cannot be applied to all types of rivers (Okhravi, 2022). In order to develop a methodology that can be applied to both gravel-bed and sand-bed rivers, a flow resistance predictor must incorporate the flow dynamics characteristics. The nondimensional hydraulic geometry approach could establish a connection between velocity distribution and the Darcy-Weisbach friction factor. This approach effectively captures the influence of bed features on flow resistance, particularly in the presence of bedforms in deep flows over sand-bed rivers in lowland areas (Cai et al., 2020; Champion and Tanner, 2000; Okhravi et al., 2022a) and moderately deep flows over gravel-bed rivers (Ferguson et al., 2017; Namaee et al., 2017; Rickenmann and Recking, 2011). The findings of this study align with this behavior, highlighting the lower accuracy of the flow resistance predictor in gravel-bed rivers (Eq. (11)), where the majority of $h/d_{84} < 10$ as observed in Table 1, and very shallow flows are characterized by large-scale roughness ($h/d_{84} < 4$ in several sections). Eq. (11) adopts a nondimensional form fitting VPE recommended by Ferguson et al. (2017) for shallow flows, where $u^{**} \propto q^{*0.6}$. However, a slight increase in the power of q^* beyond 0.6 in Eq. (11) indicates the presence of very shallow flow in the utilized dataset.

In general, the applicability of the nondimensional hydraulic geometry approach is limited to rivers that share similarities with those used to develop the regression equations. Therefore, the accuracy of the flow resistance predictor in gravel-bed rivers in mountainous areas was evaluated using a power equation based on relative submergence (Eq. (13)) from the study conducted by Afzalimehr et al. (2011). This choice was made because coarse-bed rivers in their study region, located in the central parts of Iran, exhibit physiographic similarities to the gravel-bed rivers examined in the current study. To ensure physiographic similarity, it is necessary for the variables of sediment inflow, bed and bank material, topographic features, bed slope, and channel-forming discharge to be comparable. Furthermore, the dependent variables of depth and width must be considered as a set since the flow discharge employed in the hydraulic geometry approach shapes the channel and serves as a surrogate for the dependent hydraulic parameters.

$$u^{**} = \frac{u}{u_*} = \sqrt{\frac{8}{f}} = 5.83 \left(\frac{h}{d_{84}}\right)^{0.39} \quad (13)$$

Eq. (13) showed the best fit in the study conducted by Afzalimehr et al. (2011) for coarse-bed rivers, with a standard error of 0.05 and $r^2 = 0.96$. Noteworthy, this equation was developed specifically for impervious rigid reaches with zero bed load transport. The reported Froude numbers ($0.17 < Fr < 1.17$) and relatively shallow flow conditions ($0.54 < h/d_{84} < 5.23$) within the studied rivers bear resemblance to our study (refer to Table 1, $0.18 < Fr < 0.8$ and $2.91 < h/d_{84} < 19.8$), resulting in a similar range of Darcy-Weisbach friction factor ($0.058 < f < 0.21$) in our study (see Table 1), compared to the reported range of $0.06 < f < 0.41$ in Afzalimehr et al. (2011).

Figure (4a) displays the comparison between f values predicted by the developed Eq. (11) and Eq. (13) using our field data. Approximately 53% of the results fall within the boundaries defined by the +30% and –40% lines, indicating a satisfactory predictive performance of the developed equation for gravel-bed rivers in mountainous areas. The presence of flow non-uniformity and high variability in energy slope within gravel-bed rivers diminishes the predictive performance of flow resistance based on the non-dimensional flow discharge method, while Eq. (11) takes into account all boundary resistances to flow by utilizing q^*.

The significant disparity between the predicted f values obtained from the two predictors (Fig. 4a) can be attributed to surface water variations influenced by abrupt changes in bed slope (see S in Table 1), the distribution of gravel, cobbles, and boulders elements (Okhravi and Gohari, 2020), the shape and position of large cobbles and boulders (Hodge et al., 2020; McKie et al., 2021; Nicosia et al., 2023), and their protrusion from the channel bed (Hodge et al., 2020). The study by Ferro (2018a) on the potential application of the self-similarity hypothesis to flow-resistance laws demonstrated that flow resistance depends on the Reynolds, Froude, and Shields (1936) numbers. To account for water surface distortion effects caused by boulder drag and other sources of energy extraction such as bed load transport and local hydraulic jumps, Mendicino and Colosimo (2019) incorporated the combined action of the Froude number and a modified Shields parameter suggested by Yalin (1972) into conventional flow resistance formulas, such as Eq. (2), resulting in notable improvements even for very large-scale roughness (i.e., $R/d_{84} \approx 1$). Overall, geomorphologists studying the fluvial hydraulics of coarse-bed rivers have been actively investigating the uncertainties involved in estimating water-surface profiles to better understand and address flow resistance challenges.

In the case of low-gradient sand-bed rivers, the flow resistance predictor showed excellent performance. This study demonstrated that the flow discharge-styled equation in Eq. (4), which incorporates key flow characteristics and variations in the free surface flow, can be effectively applied to predict flow resistance in river sections characterized by vegetation and dominated by lower regime flow bedforms such as dunes (over coarse sand) and ripples (over fine to medium sand).

Through regression analysis, predictors for sand-bed rivers (Eq. (12)) were derived and validated using a series of field data collected from a lowland river in the Upper Stör River catchment in Northern Germany (Song et al., 2014, 2017). The physiographic similarity between this German catchment and the

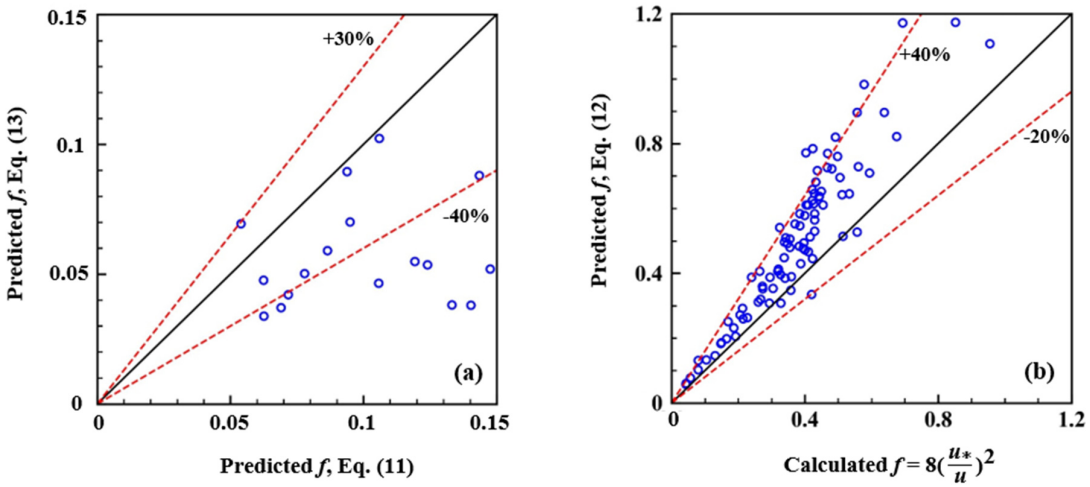


Fig. 4. Comparison of predicted *f* values using developed equations (Eqs. (11) and (12)) for gravel-bed and sand-bed rivers: field data and results reported by Song et al. (2014, 2017) for sand-bed rivers and Afzalimehr et al. (2011) for gravel-bed rivers.

present lowland catchment, along with the seasonal variations of roughness within a year, made it a suitable reference for validation purposes. A comparison between the predicted friction factor *f* using the reference equation ($f = 8(u_*/u)^2$) and the developed Eq. (12) revealed a relatively good agreement, with the data points aligning closely to the ideal 45-degree line and falling within the band of +40% overestimation (Fig. 4b). The good prediction performance of Eq. (12) can be attributed to the similarities observed in hydraulic and sediment characteristics between the two river catchments, as well as the temporal and spatial resemblance of distributed aquatic vegetation. These findings highlight the effectiveness of the flow discharge style of the VPE in providing the best fit for sand-bed rivers with high relative submergence among the reported cases.

CONCLUSION

Flow resistance in sand-bed (lowland) and gravel-bed (mountainous) rivers arises from different features. In sand-bed rivers, flow resistance is primarily influenced by bedforms and vegetation, which retard the flow and dissipate flow energy. On the other hand, gravel-bed rivers experience flow resistance due to grain particles and bedforms, resulting in reduced flow velocity. Traditional flow resistance estimation methods, such as Manning, Chezy, and Darcy-Weisbach equations, have been widely used but come with limitations. These equations often assume uniform and steady flow conditions, neglect bed load transport, and disregard the presence of vegetation, which do not accurately represent the complex situations found in natural rivers. Scientific contributions in the literature have highlighted the need for caution when using these equations, particularly for intermediate and large-scale roughness, such as shallow and very shallow flow conditions. As a result, alternative resistance relations have been proposed to address these limitations. Some of these relations are specifically designed for shallow flows, while others cover the full range of submergence, including very shallow flows. Notably, the VPE-based equations initially proposed by Ferguson (2007) and later modified by Rickenmann and Recking (2011) have shown promising improvements. Another notable approach is the nondimensional hydraulic geometry, which establishes a connection between the dimensionless unit discharge (q^*) and the dimensionless mean flow velocity (u^{**}). Numerous studies have demonstrated that the hydraulic geometry approach, which incorporates flow discharge as an input, provides an accurate fit to their data compilations.

This method was initially applied to lowland sand-bed rivers, characterized by small-scale roughness, deep flow with low sediment transport, and the presence of vegetation. The hydraulic geometry equations were modified by replacing d_{84} with flow depth *h*, resulting in a significant improvement in agreement between observed and calculated data. The scatter of the data points fell within ±20% error bands, as depicted in Fig. 3b. Furthermore, the developed flow resistance predictor was validated using a series of field data collected from a lowland river with similar physiographic characteristics. The results demonstrated the robust performance of the hydraulic geometry approach in these types of rivers, effectively capturing spatial and temporal variations in the river bed and bank conditions, as well as accounting for the influence of vegetation in small-scale roughness scenarios.

The method was subsequently evaluated in gravel-bed rivers, which are characterized by highly variable water surfaces and relatively shallow flows (large-scale roughness) over armored downstream reaches. The developed flow resistance predictor demonstrated satisfactory performance when compared to a power-form predictor derived from extensive field data sets in similar physiographic gravel-bed rivers. However, it should be noted that the validity of the predictor for gravel-bed rivers is somewhat limited due to the complex characteristics of the riverbeds in these river types. The presence of large cobbles or boulders introduces high variations in water-surface profiles, making it challenging for this method to accurately capture such dynamics in situations involving large-scale roughness. Nevertheless, it is important to recognize that flow discharge plays a crucial role in shaping channel formation and reflecting bed topography irregularities. While the method provides valuable insights into flow resistance in gravel-bed rivers, its applicability in scenarios with significant water-surface profile variations caused by the presence of large cobbles or boulders remains a challenge.

Overall, the nondimensional hydraulic geometry approach has proven to be effective in predicting flow resistance across different river styles with varying characteristics. The comprehensive statistical analysis strongly supports the arguments presented earlier. This approach offers the advantage of accounting for flow non-uniformity by explicitly considering friction slope and flow discharge, while indirectly incorporating velocity

profiles. However, it is important to acknowledge that the presence of bed load and boulders, as well as other energy extraction sources, can introduce limitations in predicting flow resistance. To address these limitations, it is recommended to incorporate additional factors such as Reynolds, Froude, and Shields numbers. These parameters take into account the influence of bed load and boulders, enabling a more precise estimation of variations in water-surface profiles and flow resistance. By considering these factors, the accuracy of predictions can be significantly improved, leading to a better understanding of flow dynamics in river systems. Improving the accuracy of hydraulic computations in channel design, particularly in determining bankfull discharge and avoiding misleading engineering judgments, is a key outcome of better addressing flow resistance through the application of the nondimensional hydraulic geometry approach.

Acknowledgements. The authors acknowledge the financial support received from the project: No. VEGA 2/0028/23 in Slovakia and the research infrastructure provided by the Faculty of Agriculture, Isfahan University of Technology in Iran (http://iut.ac.ir)

REFERENCES

Afzalimehr, H., 2010. Effect of non-uniformity of flow on velocity and turbulence intensities over a cobble-bed. Hydrol. Process., 24, 3, 331–341.

Afzalimehr, H., Gallichand, J., Jueyi, S.U.I., Bagheri, E., 2011. Field investigation on friction factor in mountainous cobble-bed and boulder-bed rivers. Int. J. Sediment Res., 26, 2, 210–221.

Afzalimehr, H., Rennie, C.D., 2009. Determination of bed shear stress in gravel-bed rivers using boundary-layer parameters. Hydrol. Sci. J., 54, 1, 147–159.

Afzalimehr, H., Singh, V.P., Najafabadi, E.F., 2010. Determination of form friction factor. J. Hydrol. Eng., 15, 3, 237–243.

Alemi, M., Maia, R., 2022. A three-step approach for bias adjustment of satellite-based daily precipitation data. In: Proc. 39th IAHR World Congress, International Association for Hydro-Environment Engineering and Research, June 19–24, Granada, Spain.

Allen, J., Somerfield, P., Gilbert, F., 2007. Quantifying uncertainty in high-resolution coupled hydrodynamic-ecosystem models. J. Mar. Syst., 64, 1–4, 3–14.

Amiri, M.J., Bahrami, M., Hamidifar, H., Eslamian, S., 2016. Modification of furrow Manning's roughness coefficient estimation by finite difference technique under surge and continuous flow. Int. J. Hydrol. Sci. Technol., 6, 3, 226–237.

Box, W., Järvelä, J., Västilä, K., 2021. Flow resistance of floodplain vegetation mixtures for modeling river flows. J. Hydrol., 601, 126593. https://doi.org/10.1016/j.jhydrol.2021.126593

Cai, R., Zhang, H., Zhang, Y., Zhang, L., Huang, H., 2020. Flow resistance equation in sand-bed rivers and its practical application in the Yellow River. Water, 12, 3, 727. https://doi.org/10.3390/w12030727

Champion, P.D., Tanner, C.C., 2000. Seasonality of macrophytes and interaction with flow in a New Zealand lowland stream. Hydrobiologia, 441, 1, 1–12.

D'Agostino, V., Michelini, T., 2015. On kinematics and flow velocity prediction in step-pool channels. Water Resour. Res., 51, 6, 4650–4667.

Dey, S., 2014. Fluvial Hydrodynamics. Hydrodynamic and Sediment Transport Phenomena. Springer, 687 p.

Dingman, S.L., 2009. Fluvial Hydraulics. Oxford University Press.

Diplas, P., Chatanantavet, P., Almedeij, J., 2016. Streambed structure, stream power, and bed load transport: A unified outlook for gravel-bed and bedrock streams. In: Proc. Int. Conf. on fluvial hydraulics (river flow 2016), July 11–14, St. Louis, USA.

Dodangeh, E., Afzalimehr, H., 2022. Incipient motion of sediment particles in the presence of bed forms under decelerating and accelerating flows. J. Hydrol. Hydromech, 70, 1, 89–102.

Einstein, H.A., Barbarossa, N.L., 1952. River channel roughness. Trans. Am. Soc. Civil Eng., 117, 1, 1121–1132.

Eslamian, S., Okhravi, S., Eslamian, F., 2019. Constructed Wetland: Hydraulic Design. Taylor and Francis Group, CRC Press, Boca Raton FL, USA, 88 p.

Ferguson, R.I., Sharma, B.P., Hardy, R.J., Hodge, R.A., Warburton, J., 2017. Flow resistance and hydraulic geometry in contrasting reaches of a bedrock channel. Water Resour. Res., 53, 3, 2278–2293.

Ferguson, R., 2007. Flow resistance equations for gravel-and boulder-bed streams. Water Resour. Res., 43, 5. https://doi.org/10.1029/2006WR005422

Ferguson, R., 2010. Time to abandon the Manning equation? Earth Surf. Process. Landf., 35, 15, 1873–1876.

Ferguson, R.I., Lewin, J., Hardy, R.J., 2022. Fluvial processes and landforms. Geol. Soc. Lond. Mem., 58, 257–270.

Ferro, V., 2018a. Assessing flow resistance in gravel bed channels by dimensional analysis and self-similarity. Catena, 169, 119–127.

Ferro, V., 2018b. Flow resistance law under equilibrium bed-load transport condition. Flow Meas. Instrum., 64, 1–8.

Franklin, P., Dunbar, M., Whitehead, P., 2008. Flow controls on lowland river macrophytes: a review. Sci. Total Environ., 400, 1–3, 369–378.

Garcia, M., Parker, G., 1993. Experiments on the entrainment of sediment into suspension by a dense bottom current. J. Geophys. Res. Oceans, 98, C3, 4793–4807.

García, M.H., 2008. Sediment transport and morphodynamics. In: García, M.H. (Ed.): Sedimentation Engineering: Processes, Measurements, Modeling, and Practice. Manuals and reports on engineering practice number 110. American Society of Civil Engineers, Reston, pp. 21–163.

Hodge, R.A., Voepel, H., Leyland, J., Sear, D.A., Ahmed, S., 2020. X-ray computed tomography reveals that grain protrusion controls critical shear stress for entrainment of fluvial gravels. Geology, 48, 2, 149–153.

Julien, P.Y., 1995. Erosion and Sedimentation. Cambridge University Press. Melbourne, USA.

Malakar, P., Das, R., 2021. Relative role of sediment entrainments on log-law parameters of longitudinal velocity distributions in mobile bed flows. J. Hydrol. Hydromech, 69, 3, 243–254.

McKie, C.W., Juez, C., Plumb, B.D., Annable, W.K., Franca, M.J., 2021. How large immobile sediments in gravel bed rivers impact sediment transport and bed morphology. J. Hydraul. Eng., 147, 2, 04020096. https://doi.org/10.1061/(ASCE)HY.1943-7900.0001842

Mendicino, G., Colosimo, F., 2019. Analysis of flow resistance equations in gravel-bed rivers with intermittent regimes: Calabrian fiumare data set. Water Resour. Res., 55, 8, 7294–7319.

Mewis, P., 2021. Estimation of vegetation-induced flow resistance for hydraulic computations using airborne laser scanning data. Water, 13, 13, 1864. https://doi.org/10.3390/w13131864

Moriasi, D., Gitau, M., Pai, N., Daggupati, P., 2015. Hydrologic and water quality models: Performance measures and evaluation criteria. Trans. ASABE (American Society of Agricultural and Biological Engineers), 58, 6, 1763–1785.

Naderi, M., Afzalimehr, H., Dehghan, A., Darban, N., Nazari-Sharabian, M., Karakouzian, M., 2022. Field study of three-parameter flow resistance model in rivers with vegetation patch. Fluids, 7, 8, 284. https://doi.org/10.3390/fluids7080284

Namaee, M.R., Sui, J., Whitcombe, T., 2017. A revisit of different models for flow resistance in gravel-bed rivers and hydraulic flumes. Int. J. River Basin Manage., 15, 3, 277–286.

Nezu, I., Nakagawa, H., 1993. Turbulence in Open Channel Flows. IAHR Monograph, A.A. Balkema, Rotterdam.

Nicosia, A., Carollo, F.G., Ferro, V., 2023. Evaluating the influence of boulder arrangement on flow resistance in gravel-bed channels. J. Hydrol., 621, 129610. https://doi.org/10.1016/j.jhydrol.2023.129610

Okhravi, S., 2022. The use of the Manning equation is not safe for different river types. What are the alternatives? In: Proc. 34th Conference of Young Hydrologists Professionals in Water Sciences. International Hydrological Program of UNESCO, Slovak Hydrometeorological Institute, November 10, Bratislava, Slovakia.

Okhravi, S., Gohari, S., 2020. Form friction factor of armored riverbeds. Can. J. Civ. Eng., 47, 11, 1238–1248.

Okhravi, S., Schügerl, R., Velísková, Y., 2022a. Flow resistance in lowland rivers impacted by distributed aquatic vegetation. Water Resour. Manage., 36, 2257–2273.

Okhravi, S., Sokáč, M., Velísková, Y., 2022b. Three-dimensional numerical modeling of water temperature distribution in the Rozgrund Reservoir, Slovakia. Acta Hydrologica Slovaca, 23, 2, 305–316.

Okhravi. S., Eslamian, S., 2022. Form resistance prediction in gravel-bed rivers. In: Eslamian, S., Eslamian, F. (Eds.): Flood Handbook. Taylor and Francis Group, CRC Press, pp. 125–138.

Powell, D.M., 2014. Flow resistance in gravel-bed rivers: Progress in research. Earth Sci. Rev., 136, 301–338.

Rickenmann, D., Recking, A., 2011. Evaluation of flow resistance in gravel-bed rivers through a large field data set. Water Resour. Res., 47, 7. https://doi.org/10.1029/2010WR009793

Schügerl, R., Velísková, Y., Sočuvka, V., Dulovičová, R., 2020. Effect of aquatic vegetation on Manning roughness coefficient value-case study at the Šúrsky channel. Acta Hydrologica Slovaca, 21, 1, 123–129.

Shields, A., 1936. Application of similarity principles and turbulence research to bedload movement. PhD Thesis. Berlin, Germany: Mitteilungen der Preussischen Versuchsanstalt für Wasserbau und Schiffbau, Technischen Hochschule Berlin. (In German.)

Song, S., Schmalz, B., Fohrer, N., 2014. Simulation and comparison of stream power in-channel and on the floodplain in a German lowland area. J. Hydrol. Hydromech., 62, 2, 133–144.

Song, S., Schmalz, B., Xu, Y.P., Fohrer, N., 2017. Seasonality of roughness-the indicator of annual river flow resistance condition in a lowland catchment. Water Resour. Manage., 31, 11, 3299–3312.

Sulaiman, M.S., Sinnakaudan, S.K., Azhari, N.N., Abidin, R.Z., 2017. Behavioral of sediment transport at lowland and mountainous rivers: a special reference to selected Malaysian rivers. Environ. Earth Sci., 76, 7, 300. https://doi.org/10.1007/s12665-017-6620-y

Thomas, C., Stamataki, I., Rosselló-Geli, J., 2023. Reconstruction of the 1974 flash flood in Sóller (Mallorca) using a hydraulic 1D/2D model. J. Hydrol. Hydromech, 71, 1, 49–63.

Van Rijn, L.C., 1984. Sediment transport, part III: bed forms and alluvial roughness. J. Hydraul. Eng., 110, 12, 1733–1754.

Vanoni, V.A., Brooks, N.H., 1957. Laboratory studies of the roughness and suspended load of alluvial streams (No. 11). US Army Engineer Division, Missouri River.

Venditti, J.G., 2013. Bedforms in sand-bedded rivers. In: Bishop, M.P., Shroder, J.F. (Eds.): Treatise on Geomorphology. Vol 3. Remote Sensing and GIScience in Geomorphology. Elsevier Academic Press.

Willemsen, P.W., Horstman, E.M., Bouma, T.J., Baptist, M.J., Van Puijenbroek, M.E., Borsje, B.W., 2022. Facilitating salt marsh restoration: the importance of event-based bed level dynamics and seasonal trends in bed level change. Front. Mar. Sci., 8, 793235. https://doi.org/10.3389/fmars.2021.793235

Willmott, C.J., Robeson, S.M., Matsuura, K., 2012. A refined index of model performance. Int. J. Climatol, 32, 13, 2088–2094.

Wright, S., Parker, G., 2004. Flow resistance and suspended load in sand-bed rivers: simplified stratification model. J. Hydraul. Eng., 130, 8, 796–805.

Yalin, M.S., 1972. Mechanics of Sediment Transport. 1st Ed. Pergamon Press, Oxford, Toronto.

Yang, S.Q., Tan, S.K., Lim, S.Y., 2005. Flow resistance and bed form geometry in a wide alluvial channel. Water Resour. Res., 41, 9. https://doi.org/10.1029/2005WR004211

Yen, B.C., 2002. Open channel flow resistance. J. Hydraul. Eng., 128, 20–39.

Zomer, J.Y., Vermeulen, B., Hoitink, A.J., 2023. Coexistence of two dune scales in a lowland river. Earth Surf. Dynam. Discuss. (Preprint). https://doi.org/10.5194/esurf-2023-12. (In review)

Zwolenik, M., Michalec, B., 2023. Effect of water surface slope and friction slope on the value of the estimated Manning's roughness coefficient in gravel-bed streams. J. Hydrol. Hydromech, 71, 1, 80–90.

Received 30 March 2023
Accepted 15 June 2023